Efficient 2.87 μm fiber laser passively switched using a semiconductor saturable absorber mirror

Jianfeng Li,[1,2,*] Darren D. Hudson,[1] Yong Liu,[2] and Stuart D. Jackson[1]

[1]*Institute of Photonics and Optical Science and Centre for Ultrahigh bandwidth Devices for Optical Systems (CUDOS), School of Physics, University of Sydney, Camperdown 2006, Australia*

[2]*State Key Laboratory of Electronic Thin Films and Integrated Devices, School of Optoelectronic Information, University of Electronic Science and Technology of China (UESTC), Chengdu 610054, China*

**Corresponding author: lijianfeng@uestc.edu.cn*

Received April 20, 2012; revised August 1, 2012; accepted August 2, 2012; posted August 3, 2012 (Doc. ID 167210); published September 5, 2012

A passively switched Ho^{3+}, Pr^{3+} codoped fluoride fiber laser using a semiconductor saturable absorber mirror (SESAM) is demonstrated. Q-switching and partial mode-locking were observed with the output power produced at a slope efficiency of 24% with respect to the absorbed pump power. The partially mode-locked 2.87 μm pulses operated at a repetition rate of 27.1 MHz with an average power of 132 mW, pulse energy of 4.9 nJ, and pulse width of 24 ps. © 2012 Optical Society of America

OCIS codes: 140.3510, 140.4050.

Pulsed fluoride glass fiber lasers operating in the mid-infrared region have attracted significant attention because of their potential applications in defense, laser microsurgery, and mid-infrared photonics. Fluoride glass pulsed fiber lasers have been reported based on Er^{3+}-doped and Er^{3+}, Pr^{3+} codoped fluoride fibers [1–5]. Recently, we have extended this work by creating actively Q-switched cascaded 380 and 260 ns pulses at 3.005 and 2.074 μm, respectively, using singly Ho^{3+}-doped ZBLAN fiber [6] and 78 ns actively Q-switched pulse widths at 2.86 μm using Ho^{3+}, Pr^{3+} codoped ZBLAN fiber at a comparatively high slope efficiency of 20% [7].

Compared to Q-switched fiber lasers, mode-locked fiber lasers are particularly useful because they typically offer a higher peak power and a significantly shorter pulse width that can be used to pump optical parametric oscillators or to create a supercontinuum in the mid-infrared region. In the past few years, several passively mode-locked fiber lasers emitting at 2 μm have been reported, with the best performance being achieved with thulium-doped silicate fiber that produced 1.5 ps duration pulses and 0.76 nJ pulse energies using semiconductor saturable absorber mirrors (SESAMs) [8], and with dispersion compensation, 173 fs stretched-pulses with 4 nJ pulse energy was obtained at 1.97 μm [9].

Compared to Er^{3+}-doped ZBLAN fiber lasers, Ho^{3+}-doped ZBLAN fiber lasers have a longer emission peak wavelength and a higher Stokes efficiency limit as a result of the longer pump wavelength of 1150 nm. In a similar way to the transition in Er^{3+}-doped ZBLAN, the $^5I_6 \rightarrow {}^5I_7$ laser transition of Ho^{3+} encounters a potential population bottlenecking problem because the 3.5 ms lifetime of the upper ($^5I_6$) laser level is shorter than the 12 ms lifetime of the lower ($^5I_7$) laser level and, in a parallel way to Er^{3+}, Ho^{3+} requires some engineering of the doping or laser process in order to create efficient emission. For example, quenching of the $^5I_7$ lifetime by Pr^{3+} codoping has resulted in efficient cw [10] and actively Q-switched pulsed operation [7].

In this Letter, we report the demonstration of a passively Q-switched and partially mode-locked Ho^{3+}, Pr^{3+} codoped fluoride laser that produced pulses at 2.87 μm using newly developed SESAM. Q-switching, Q-switched mode-locking, and unstable cw mode-locking regimes was observed with increasing pump power.

The experimental arrangement for the passively switched Ho^{3+}, Pr^{3+} codoped ZBLAN fiber laser is shown in Fig. 1. The double-clad fluoride fiber (FiberLabs, Japan) was identical to the fiber used in our previous free-running experiment [10] and had a D-shaped pump core with a diameter of 125 μm across the circular cross section and a numerical aperture (NA) of 0.50. The fiber had a 10 μm-core diameter with an NA of 0.2. The Ho^{3+} and Pr^{3+} ion concentrations of the fiber were 30,000 and 2,500 ppm molar, respectively. The selected fiber length of 3.5 m provided 88% pump absorption efficiency.

Commercially available high power 1.15 μm diode lasers (Eagleyard Photonics, Berlin) were used to pump the fiber after polarization multiplexing and focusing using an antireflection-coated ZnSe objective lens (Innovation Photonics, LFO-5-6-3.0 μm, 0.25 NA) which also collimated the 2.87 μm output that was emitted from the fiber core. A highly pump-transmitting dichroic mirror with a reflectivity of >98% between 2.5 and 3.2 μm was positioned between the polarizing beam splitter and a focusing lens and placed at an angle of 15° with respect to the pump beam, was used to direct the fiber laser output. The other end of the fiber was cleaved at an angle of 8° to avoid parasitic lasing. Two ZnSe objective

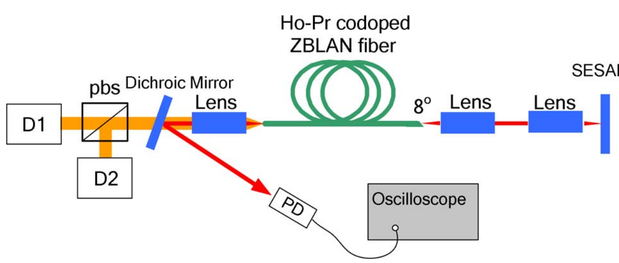

Fig. 1. (Color online) Schematic of the experiment setup. D1-D2 represents the pump diodes, pbs represents the polarizing beam splitter, and PD represents the photodetector.

lenses were used to collimate and focus the emission from the angled fiber end onto to the SESAM, which provided the saturable absorption required to start and maintain the passive switching of the laser. The GaAs-based SESAM (BATOP GmbH) provided a high reflectivity ($R > 60\%$) from 2.8 to 3.4 μm with an unsaturated loss of 15%, a modulation depth of 18%, a nominal recovery time of ~1 ps, and a damage threshold of 350 MW cm^{-2}.

For the measurements of the laser output, an InAs photodetector with a response time of approximately 2 ns was connected to a 1 GHz digital oscilloscope which was used to measure the pulse train and pulse waveforms. The pulse duration during partial mode-locking was measured by a two-photon intensity autocorrelator. A calibrated monochromator (with 0.3 nm resolution) that employed a thermoelectrically cooled InAs photodiode spectrum was used to measure the laser spectrum at 3 μm.

In a way that is typical of passively mode-locked lasers using SESAMs, we observed that the fiber laser went through several operating regimes as the pump power was increased. The threshold launched pump power for cw operation was 56.5 mW. After reaching the launched pump power of 155 mW, *Q*-switched pulses were observed as a result of the relatively high modulation depth of the SESAM. Figure 2 shows the repetition rate and pulse width as a function of the launched pump power. As expected, the repetition rate increases and pulse width decreases with the increased launched pump power. The narrowest pulse duration of 720 ns that was produced with an average output power of 54 mW was achieved at a launched pump power of 313 mW. The average pulse energy was calculated to be 1.1 μJ. The inset to Fig. 2 shows the measured *Q*-switched pulses at a launched pump power of 313 mW. The pulse-to-pulse amplitude stability of the *Q*-switched pulse was approximately ±10%.

By increasing the launched pump power to 320 mW, *Q*-switched mode-locking operation was achieved; see Fig. 3(a). Operation in this regime, however, occurred within a very narrow pump power range. CW mode-locking was observed when the launched pump power was increased to 360 mW, as shown in Fig. 3(b). The repetition rate was measured to be 27.1 MHz using an rf

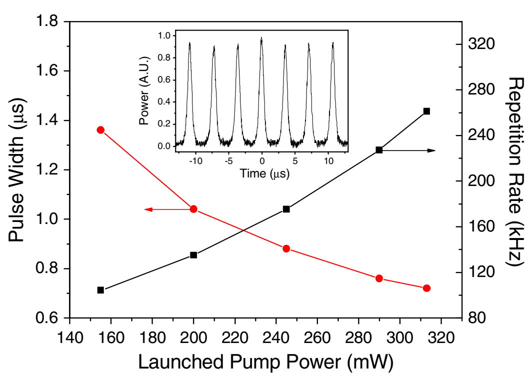

Fig. 2. (Color online) Measured pulse width and repetition rate as a function of the launched pump power in the passively *Q*-switching regime.

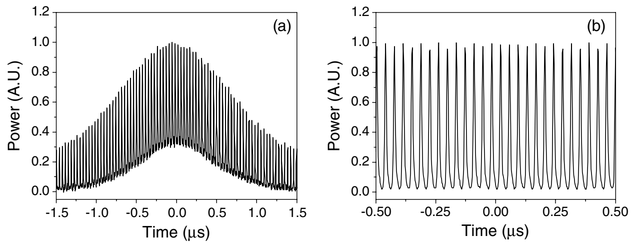

Fig. 3. Measured output pulse train in (a) *Q*-switched mode-locking and (b) cw mode-locking regimes.

spectrum analyzer, which was equal to the calculated value according to the cavity length. The signal-to-noise ratio of the rf beat was typically 50 dB instead of the 60–80 dB usually observed in stable mode-locked lasers. Thus, the mode-locking in this system appears to be a partial or unstable mode-locking; the amplitudes in the rf beat spectrum at times also displayed indications of multiple pulsing. This is perhaps not surprising given that the system was not optimized for mechanical or thermal stability, and some residual back-reflection from the angle-cleaved fiber tip was observed.

The average power of the partially mode-locked pulses increased with the launched pump power and attained the maximum value of 132 mW at a launched pump power of 685 mW. The average pulse energy was calculated to be 4.9 nJ. Mode-locking ceased when the launched pump power was increased beyond 685 mW and returned when the pump was reduced below this level, which indicated that the SESAM was not damaged. The loss of partial mode-locking at higher pump power may result from the onset of two photon absorption which is nonsaturable.

Figure 4 shows the optical spectrum of the output for cw operation with the SESAM replaced by a mirror with reflectivity of >98% between 2.5 and 3.2 μm, and cw mode-locked pulsed operation using the SESAM at a launched pump power of 685 mW. The free-running laser operated at a center wavelength of 2.872 μm and bandwidth of 4 nm; under mode-locked conditions, the center wavelength shifted to 2.870 μm due to the lower feedback of SESAM and the bandwidth was essentially unchanged.

The optical pulse width was measured using an in-house interferometric autocorrelator, as shown in Fig. 5. Two-photon absorption in an InGaAs photodiode was used for detection. To prevent residual pump and room

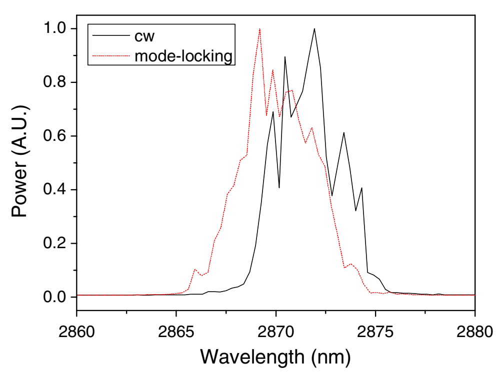

Fig. 4. (Color online) Measured spectrum for cw and mode-locked pulsed operation at launched pump power of 685 mW.

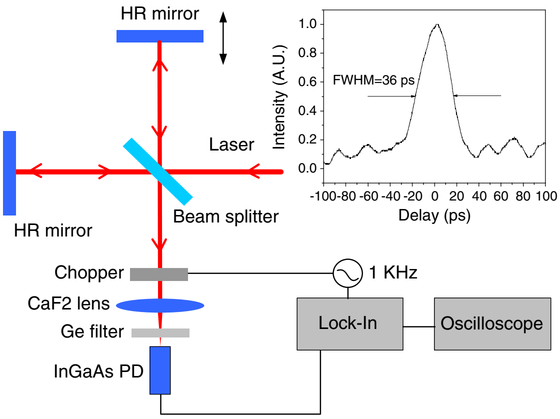

Fig. 5. (Color online) Schematic of the layout of the intensity autocorrelator and the autocorrelation trace at 132 mW average output power. The mode-locked pulses are 24 ps in duration. The oscillations on the edges of the autocorrelation correspond to background noise on the detection system and not to an optical signal.

light from interfering with the measurement, a germanium filter was placed in front of the detector. An optical beam chopper and lock-in amplifier were used to accurately measure the weak two-photon signal from the InGaAs photodiode. The envelope of the intensity autocorrelation for pulses at an average output power of 132 mW is shown in Fig. 5. The FWHM of the autocorrelation trace was 36 ps. Assuming that the envelope of the intensity autocorrelation approximated a sech pulse shape, this yields an FWHM pulse width of 24 ps. Since this system is partially mode-locked, one might expect the autocorrelation to show the broad pedestal typical of noise-burst autocorrelations. However, we cannot claim that the autocorrelation shown in Fig. 5 is pedestal free since it is likely that a low intensity pedestal would be below the noise floor of our autocorrelator.

The center emission wavelength of 2.87 μm, peak power of 206 W, and pulse width of 24 ps are encouraging results which compare favorably with the pioneering demonstration of a mode-locked 2.7 μm Er^{3+}-doped fluoride fiber laser [2] which involved the use of either a moving mirror or InAs epilayers deposited on a GaAs substrate for saturable absorption. In both modes of operation, Q-switched mode-locking was produced and the maximum peak power of the Q-switched pulse envelope was approximately 4 W. While the pulse widths of our partial mode-locked laser are quite long compared to many past demonstrations of mode-locked fiber lasers that use SESAM, no attempt was made to balance the intracavity dispersion. As has been observed in a previously demonstrated mode-locked Yb^{3+}-doped fiber laser [11], uncompensated intracavity dispersion creates pulses that have significantly longer duration than the limit imposed by the recovery time of the SESAM. The ZBLAN fiber used here presents anomalous dispersion ($-0.087\ \mathrm{ps}^2\ \mathrm{m}^{-1}$) at 2.87 μm [12]. Thus, by adding normal dispersion to the cavity, e.g., via a grating telescope [13], we can expect shorter output pulses. In the current system, the time-bandwidth product is 3.5, more than 10 times the fundamental limit for sech pulses. Thus, with optimized dispersion, the fluoride fiber laser should produce pulses down to approximately 2 ps duration, and with improved mechanical and thermal stability, stable mode-locked operation at 2.87 μm is envisaged; minimization of back reflections from the intracavity fiber tip and free-space components will further stabilize mode-locking. To achieve high resolution and high signal-to-noise autocorrelations, a future embodiment of the autocorrelator will involve a high-gain InGaAs photodiode and a high precision translation stage.

In summary, we have demonstrated passive switching of a Ho^{3+}, Pr^{3+} codoped fluoride fiber laser using a GaAs SESAM. We observed Q-switched pulses with 720 ns duration for a pump power of 313 mW, and partially mode-locked pulses with durations of 24 ps for a pump power of 685 mW. The maximum average power of the partially mode-locked system was 132 mW, yielding pulse energies of 4.9 nJ. The pulse width of 24 ps is the shortest reported pulse width from a fiber laser operating in this wavelength range, and could lead to a range of applications involving large electric field interactions with molecules. Further increases in the average power and the reduction of the pulse duration are expected with the incorporation a fluoride-based amplifier and compensation of the intracavity dispersion, respectively.

The authors acknowledge financial support from the Australian Research Council through the Discovery Projects funding scheme. This research was conducted in part by the Australian Research Council Centre of Excellence for Ultrahigh bandwidth Devices for Optical Systems (project No. CE110001018). S. J. acknowledges support from a Queen Elizabeth II Fellowship. This work was also supported by National Nature Science Foundation of China (Grant Nos. 61107037 and 60925019), China Postdoctoral Science Special Foundation (Grant No. 201003693), and the Fundamental Research Funds for the Central Universities (Grant No. ZYGX2009J053).

References

1. C. Frerichs and U. B. Unrau, Opt. Fiber Technol. **2**, 358 (1996).
2. N. Libatique, J. Tafoya, S. H. Feng, D. Mirell, and R. Jain, in *Advanced Solid State Lasers*, OSA Technical Digest Series (Optical Society of America, 2000), paper MD2.
3. T. Segi, K. Shima, T. Sakai, and H. Hosoya, in *Conference on Lasers and Electro-Optics (CLEO)*, OSA Technical Digest (Optical Society of America, 2004), paper CThZ5.
4. M. Gorjan, R. Petkovšek, M. Marinček, and M. Čopič, Opt. Lett. **36**, 1923 (2011).
5. S. Tokita, M. Murakami, S. Shimizu, M. Hashida, and S. Sakabe, Opt. Lett. **36**, 2812 (2011).
6. J. Li, T. Hu, and S. D. Jackson, Opt. Lett. **37**, 228 (2012).
7. T. Hu, D. D. Hudson, and S. D. Jackson, Opt. Lett. **37**, 2145 (2012).
8. Q. Wang, J. Geng, T. Luo, and S. Jiang, Opt. Lett. **34**, 3616 (2009).
9. F. Haxsen, A. Ruehl, M. Engelbrecht, D. Wandt, U. Morgner, and D. Kracht, Opt. Express **16**, 20471 (2008).
10. S. D. Jackson, Opt. Lett. **34**, 2327 (2009).
11. L. A. Gomes, L. Orsila, T. Jouhti, and O. G. Okhotnikov, IEEE J. Sel. Top. Quantum Electron. **10**, 129 (2004).
12. F. Gan, J. Non-Cryst. Solids **184**, 9 (1995).
13. M. Engelbrecht, F. Haxsen, A. Ruehl, D. Wandt, and D. Kracht, Opt. Lett. **33**, 690 (2008).